Theoretical Study of Hydroxyisoprene Alkoxy Radicals and Their Decomposition Pathways

Wenfang Lei and Renyi Zhang*

Department of Atmospheric Sciences, Texas A&M University, College Station, Texas 77843

Received: November 9, 2000; In Final Form: January 31, 2001

We report theoretical studies of the alkoxy radicals arising from the OH-initiated reactions of isoprene and their decomposition pathways. Density functional theory (DFT) and ab initio molecular orbital calculations have been employed to determine the structures and energies of the alkoxy radicals as well as the transition states and products of their decomposition reactions. Geometry optimizations of the various species were performed with density functional theory at the B3LYP/6-31G(d,p) level, and the single-point energies were computed using various methods, including second-order Møller–Plesset perturbation theory (MP2) and the coupled-cluster theory with single and double excitations including perturbative corrections for the triple excitations (CCSD(T)). The ab initio energetics of the alkoxy radicals along with their transition states and products of decomposition were used to determine the reaction and activation enthalpies of the C–C bond fission of the alkoxy radicals. The results indicate that the calculated energies are very sensitive to the electron correlation effect. For example, at the CCSD(T)/6-311G(d,p) level of theory, decomposition of the β-hydroxyalkoxy radical with OH and O$^\bullet$ located at C1 and C2 (respectively) is found to be slightly endothermic (by 2.1 kcal mol^{-1}), with an activation barrier of 8.5 kcal mol^{-1}. Those values are noticeably different from the results obtained using the MP2 and B3LYP methods. Using the obtained activation barriers and the transition state structures, we have calculated the high-pressure limit decomposition rates of the various isomers of the alkoxy radicals. The C–C bond fission is expected to occur readily for the four β-hydroxyalkoxy radicals with the calculated rate constants in the range of 4×10^7 to 6×10^8 s^{-1}, but the rates are much lower for the two δ-hydroxyalkoxy radicals ($<3 \times 10^{-2}$ s^{-1}).

Introduction

Isoprene (2-methyl-1,3-butadiene, CH$_2$=C(CH$_3$)CH=CH$_2$) is one of the most abundant hydrocarbons emitted by the terrestrial biosphere, with a global averaged production rate of about 450 Tg yr^{-1},[1] and is sufficiently reactive to influence oxidation levels over large portions of the continental troposphere.[2,3] Due to its high chemical reactivity and proliferation in the generation of peroxy radicals,[4,5] isoprene plays an important role in ozone formation in local and regional atmosphere.[6,7]

The atmospheric oxidation of isoprene is mainly initiated by an attack from the hydroxyl radical OH, the dominant tropospheric removal pathway for isoprene. The reaction between isoprene and OH occurs by OH addition to the >C=C< bonds, forming four possible thermodynamically favored hydroxyalkyl radicals,

$$OH\bullet + C_5H_8 \rightarrow C_5H_8OH\bullet \qquad (1)$$

Under atmospheric conditions, the hydroxyalkyl radicals react with oxygen molecules to form the hydroxyalkyl peroxy radicals,[4,5]

$$C_5H_8OH\bullet + O_2 \rightarrow C_5H_8OHO_2\bullet \qquad (2)$$

Addition of O$_2$ occurs only at the carbons β to the OH position for the OH–isoprene adducts of internal OH addition but takes places at two centers (β or δ to the OH position) for the OH–isoprene adducts of terminal OH addition. Hence O$_2$ addition to the OH–isoprene adduct leads to the formation of four β-

and two δ-hydroxyperoxy radicals. Subsequent reactions of the hydroxyperoxy radicals with NO lead to the formation of four β- and two δ-hydroxyalkoxy radicals,

$$C_5H_8OHO_2\bullet + NO \rightarrow C_5H_8OHO\bullet + NO_2 \qquad (3)$$

Under atmospheric conditions, the hydroxyalkoxy radicals may undergo decomposition, isomerization, or reaction with O$_2$, yielding various oxygenated organic compound.[4] Figure 1 shows the likely decomposition pathways for the six isomers of the alkoxy radicals.

Currently, there is considerable uncertainty concerning the fate of the intermediate radicals formed during the isoprene oxidation.[8] For example, the alkoxy radicals are the key intermediates in the isoprene oxidation reactions and have not been detected analytically.[9] On the basis of the the analysis of product distributions of the OH–isoprene reaction system in the environmental smog chamber experiments, some mechanisms of the alkoxy radical degradation pathways have been postulated. For example, it has been suggested that radicals **I** and **IV** may undergo C–C bond fission to form methyl vinyl ketone (MVK) and methacrolein (MACR), respectively, along with $\bullet$CH$_2$OH.[10–13] The $\bullet$CH$_2$OH radical subsequently reacts with O$_2$ to form formaldehyde and HO$_2$. Radicals **II** and **III** can decompose to form formaldehyde and the respective radicals; the radical products further react with O$_2$ to produce MVK or MACR, respectively. Those earlier studies also suggest that radicals **II** and **III** may undergo cyclization to produce 3-methyl furan.[10,12,13] In addition, on the basis of the identification of some carbonyl compounds formed from the OH–isoprene reactions,[14] Jeffries and coauthors propose that radical
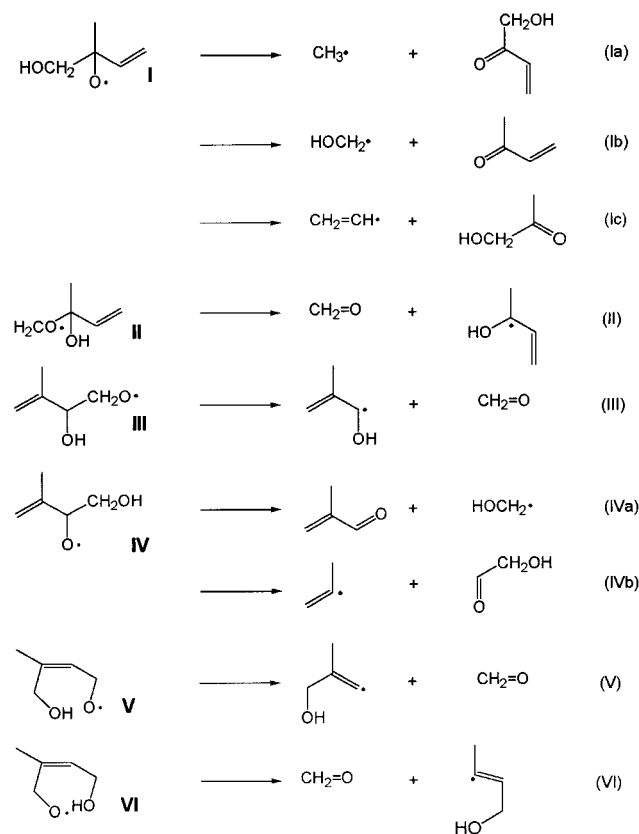
Figure 1. Schematic representation of the decomposition pathways of the hydroxyisoprene alkoxy radicals.

I may decompose to form the methyl radical and hydroxymethyl vinyl ketone, $C_4H_6O_2$. Those latter authors also suggest that the C−H fission at the α-carbon of radical **IV** results in the formation of $C_5H_6O_2$.[14] The results obtained from the earlier smog chamber investigations have been incorporated into mechanistic models of atmospheric isoprene degradation.[13,15−17] Very recently, a theoretical study has investigated the C−C fission pathways of the hydroxyisoprene alkoxy radicals and provided insight into the fate of the alkoxy radicals.[18] On the basis of ab initio calculations, Dibble concludes that the barrier to C−C bond cleavage between the α and β carbons is very small (only ∼2 kcal mol⁻¹), indicating that the unimolecular dissociation of the β-hydroxyalkoxy radical is the dominant process.

In this study, we report density functional theory (DFT) and ab initio calculations of the alkoxy radicals from the OH-initiated reactions of isoprene. The geometries and energetics of the six isomers of the alkoxy radicals are presented. We also examine the effects of electron correlation and basis set on the reaction and activation enthalpies of C−C bond fission of the alkoxy radicals. A computationally efficient method for determination of the energetics of the hydroxyisoprene alkoxy radicals is evaluated. In addition, we have calculated the rate constants of the alkoxy radical decomposition, using the presently obtained activation barriers and the transition state theory (TST). Atmospheric implications of the present results are discussed.

Theoretical Method

The theoretical computations were performed on an SGI Origin 2000 supercomputer using the Gaussian 98 software package.[19] All radicals were treated with the unrestricted Hartree−Fock (UHF) formulation. Geometry optimization was executed using Becke's three-parameter hybrid method employ-
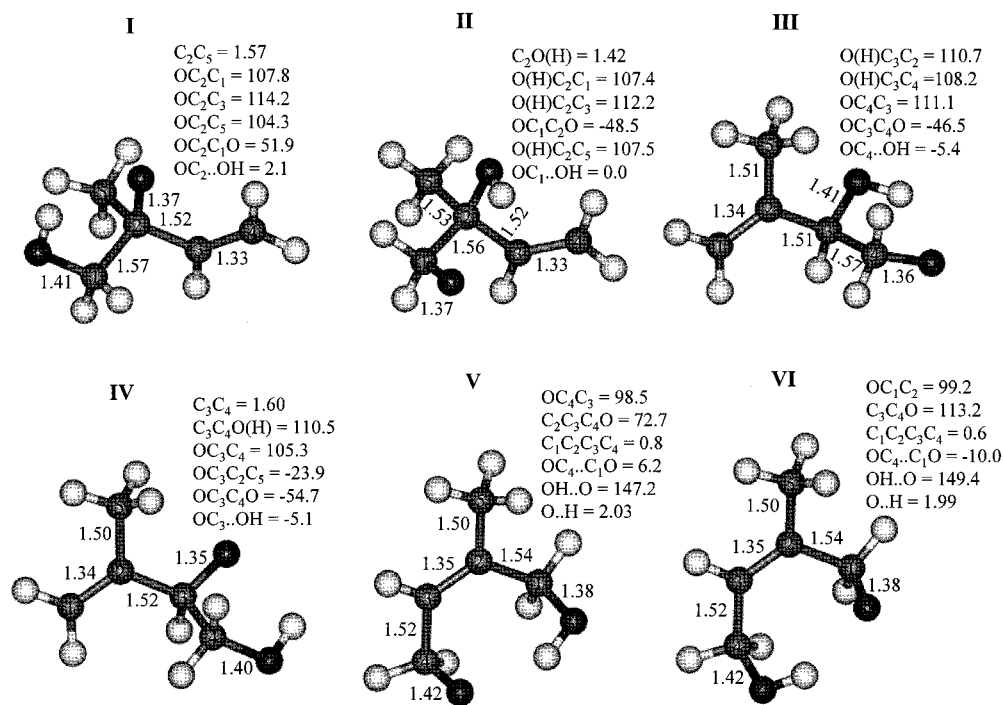
ing the LYP correction function (B3LYP) in conjunction with the split valence polarized basis set 6-31G(d,p). The DFT structures were then employed in single-point energy calculations using frozen core second-order Møller−Plesset perturbation theory (MP2) and coupled-cluster theory with single and double excitations including perturbative corrections for the triple excitations (CCSD(T)) with various basis sets. Harmonic vibrational frequency calculations were made using B3LYP/6-31G(d,p).

Recently, we have evaluated the level of ab initio theory that applies to complex organic radical species, on the basis of computational efficiency and accuracy.[20] For a set of organic radicals, we have performed full geometry optimization and energy calculations using different basis sets and levels of electron correlation and compared the results to limited available experimental data. The results indicate that electron correlation did not affect the geometries of these radicals appreciably. Better convergence behavior and considerably higher computational efficiency were achieved using the gradient density functional (NLDFT) as the method of geometry and frequency calculations. Also, it is noticed that beyond the split valence polarized level of description there was little improvement in the molecular geometry when the size of the basis set was further increased (i.e., triple split, diffuse functions, expansion of the polarization portion of the basis sets, etc.). In addition, we have investigated analogous reactions of OH addition to isoprene and subsequent O_2 addition to the OH−isoprene adduct.[20,21] Those studies indicate that the calculated energetics are very sensitive to effects of basis set and electron correlation.

For the hydroxyisoprene alkoxy radicals, single-point energy calculations at the CCSD(T) level of theory using a larger basis set (e.g. 6-311++G(d,p)) are computationally prohibitive. We have corrected basis set effects on the calculated energies for the isomers of the alkoxy radicals, on the basis of an approach that has been recently developed and employed to investigate the energetics for the OH−isoprene adduct isomers.[20] The procedure involves determination of a correction factor associated with basis set effects at the MP2 level and subsequent correction to the energy calculated at a higher level of electron correlation with a moderate size basis set. For the isomers of the alkoxy radicals, the basis set effects on the energies were evaluated at the MP2 level. A correction factor, CF, was determined from the energy difference between the MP2/6-31G(d) and MP2/6-311++G(d,p) levels. The values of calculated energies at the CCSD(T)/6-31G(d) level were then corrected by the MP2 level correction factors. For the OH−isoprene adduct radicals, this method was validated by comparing the CCSD(T) results corrected with the basis set factors to those calculated directly for the equivalent basis set.[20] In this work, we have carried out calculations with CCSD(T)/6-311G(d,p) to verify the energies obtained using the basis set correction approach.

Results and Discussion

Structures and Energetics of Alkoxy Radicals. We have recently investigated the structures and energetics of the OH−O_2−isoprene peroxy radicals.[21] In the present work we considered the equilibrium structures of those peroxy radicals to obtain the initial guesses for the corresponding alkoxy radicals. Geometry optimizations of the alkoxy radicals were initially performed using the same geometries as those of the peroxy radicals except with an oxygen atom removed. For each structural isomer, we performed additional calculations to explore possible rotational conformers. The number of rational

I

$C_2C_5 = 1.57$
$OC_2C_1 = 107.8$
$OC_2C_3 = 114.2$
$OC_2C_5 = 104.3$
$OC_2C_1O = 51.9$
$OC_2..OH = 2.1$

II

$C_2O(H) = 1.42$
$O(H)C_2C_1 = 107.4$
$O(H)C_2C_3 = 112.2$
$OC_1C_2O = -48.5$
$O(H)C_2C_5 = 107.5$
$OC_1..OH = 0.0$

III

$O(H)C_3C_2 = 110.7$
$O(H)C_3C_4 = 108.2$
$OC_4C_3 = 111.1$
$OC_3C_4O = -46.5$
$OC_4..OH = -5.4$

IV

$C_3C_4 = 1.60$
$C_3C_4O(H) = 110.5$
$OC_3C_4 = 105.3$
$OC_3C_2C_5 = -23.9$
$OC_3C_4O = -54.7$
$OC_3..OH = -5.1$

V

$OC_4C_3 = 98.5$
$C_2C_3C_4O = 72.7$
$C_1C_2C_3C_4 = 0.8$
$OC_4..C_1O = 6.2$
$OH..O = 147.2$
$O..H = 2.03$

VI

$OC_1C_2 = 99.2$
$C_3C_4O = 113.2$
$C_1C_2C_3C_4 = 0.6$
$OC_4..C_1O = -10.0$
$OH..O = 149.4$
$O..H = 1.99$

Figure 2. Optimized geometries of the six isomers of the hydroxyisoprene alkoxy radicals calculated at the B3LYP/6-31G(d,p) level of theory (bond lengths in Å and angles in deg).

conformers considered was between 7 and 12 for alkoxy radicals **I**−**IV**. Due to the possible cis and trans configurations for radicals **V** and **VI**, the number of possible rotational conformations considered was much larger (22 and 17, respectively). The cis conformations are more stable than the trans confirmations for radicals **V** and **VI**, by about 4 kcal mol^{-1}. A total of 79 rotational conformations of the alkoxy radicals were considered, and we report only the lowest rotational conformer found for each structural isomer. The lowest-energy conformers of the six alkoxy radicals are illustrated in Figure 2, obtained at the B3LYP/6-31G(d,p) level of theory. The evaluation of the vibrational frequencies confirmed that all geometries reported here represent minima on the potential energy surfaces. The total energies of the hydroxyisoprene alkoxy radicals were determined with the B3LYP/6-31G(d,p) optimized geometries using MP2 and CCSD(T) with different basis sets. The results of the total energies are summarized in Table 1. Spin contamination associated with the B3LYP optimized geometries of the six alkoxy radical isomers is minimal. The calculated spin eigenvalues, $\langle S^{**}2\rangle$, are less than 0.757 before spin projection. After the $S + 1$ component is annihilated, the values of $\langle S^{**}2\rangle$ are reduced to 0.750 (which is identical to the exact value of a pure doublet), indicating that contamination of the unrestricted Hartree−Fock wave function from higher spin states is negligible for the alkoxy radicals.
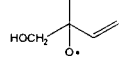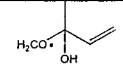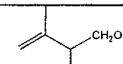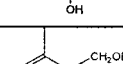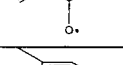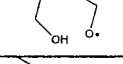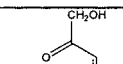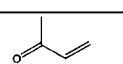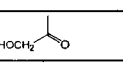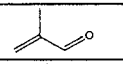
It is interesting to compare the equilibrium geometries of the alkoxy radicals shown in Figure 2 to those of the OH−O$_2$−isoprene peroxy radicals that we recently reported.[21] For the six alkoxy radicals, removal of an oxygen atom from the peroxy radical results in a shortening of the C−O• bond, but a lengthening of the C−C bonds adjacent to the radical center. The C−O• bond length of the alkoxy radicals ranges from 1.35 to 1.42, by 0.05 to 0.14 Å shorter than that of the C−O(O) bond of the corresponding peroxy radicals. The increased C−C bond length adjacent to the radical center after the O-atom removal reflects an increased σ character, as electron density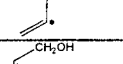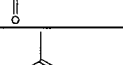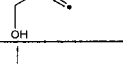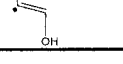 in the π bond is transferred to the strengthened C−O• bond. The C−O(H) bond length is nearly unchanged with the removal

of the O atom, except for radical **V** with a reduced C−O(H) bond length by 0.05 Å. Another interesting structural feature of the alkoxy radicals shown in Figure 2 is the existence of an intramolecular hydrogen bond to form a ring structure from the hydroxyl group to the radical center. For example, for radicals **I**−**IV**, there is a five-member ring forming from the hydroxyl group to the radical center; the length of the hydrogen bond ranges from 2.0 to 2.3 Å. Note that the O−H and C−O• bonds are nearly parallel to each other, due to the constrains imposed by the ring formation. For radicals **V** and **VI**, the hydrogen bond involves a seven-member ring structure and the hydrogen bond length is about 2 Å, somewhat shorter than those of radicals **I**−**IV**. Also for radicals **V** and **VI**, the C−O(H) and C−O• bonds are nearly parallel to each other, due to the ring formation.

Recently, a theoretical study has reported the equilibrium structures of the hydroxyisoprene alkoxy radicals obtained at B3LPY/6-311G(2df,2p) level of theory.[18] For radicals **I**−**IV**, our obtained equilibrium structures are very close to those reported previously. For radicals **V** and **VI**, although the two sets of results are still similar, there are slightly differences. For example, we obtained the hydrogen bond lengths of 2.03 and 1.99 Å for **V** and **VI**, respectively, slightly larger than the values reported previously. We have performed additional geometry optimizations by constraining a shorter length for the hydrogen bond, but after the geometry relaxation the slightly longer lengths of the hydrogen bond were still favorable.

Decomposition of Alkoxy Radicals. The decomposition pathways of the alkoxy radicals were investigated by examining the energetics of the corresponding transition states and products. The transition states of the C−C bond fission of the alkoxy radicals were identified using the relaxed potential energy scan (PES) method along the reaction coordinator. We performed constrained geometry optimizations at fixed C−C bond lengths using the B3LYP/3-21G(d) method. The C−C bond length was successfully increased from −0.3 to 1.4 Å relative to the equilibrium C−C bond length of the corresponding alkoxy radical, with an interval of 0.2 Å. Once this bond length with the energy maximum was located along the reaction coordinate,

Hydroxyisoprene Alkoxy Radicals

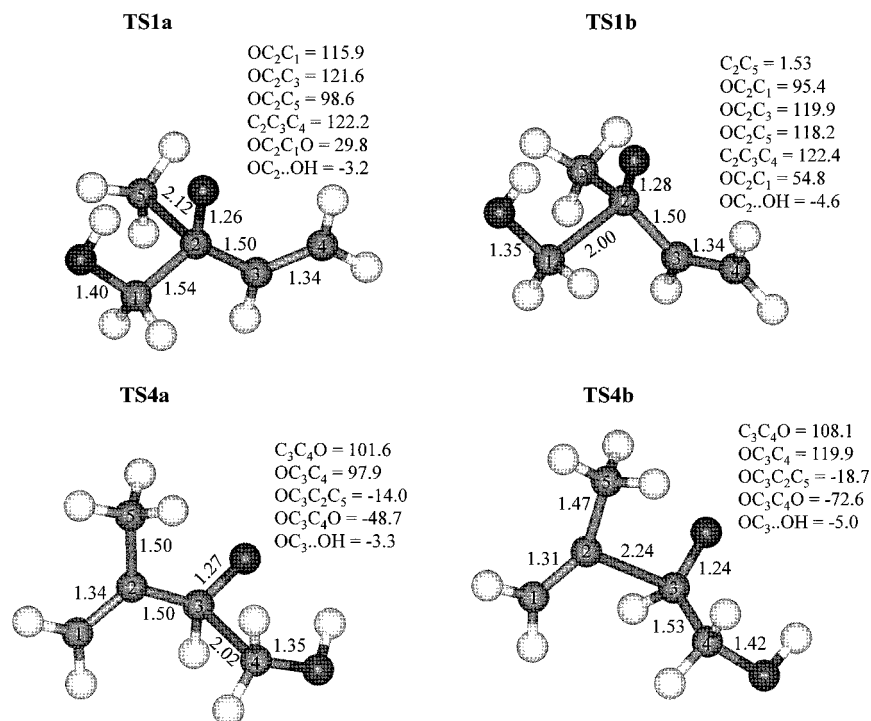*J. Phys. Chem. A, Vol. 105, No. 15, 2001* **3811**

TABLE 1: Absolute Energies and Zero-Point Energies (ZPE) (in hartrees) of Alkoxy Radicals and Their Transition States and Products of Decomposition

Species	B3LYP/6-31G(d,p)	MP2/6-31G(d)	MP2/6-311++G(d,p)	CCSD(T)/6-31G(d)	ZPE
I	-346.308302	-345.183644	-345.417880	-345.286783	0.133021
II	-346.308397	-345.187080	-345.420319	-345.288044	0.132184
III	-346.309786	-345.183700	-345.417697	-345.285171	0.132552
IV	-346.309430	-345.178898	-345.414057	-345.282955	0.132248
V	-346.306007	-345.172427	-345.406510	-345.279647	0.134592
VI	-346.304862	-345.170540	-345.404686	-345.278567	0.134408
TSIa	-346.287829	-345.146022	-345.383105	-345.259738	0.129705
TSIb	-346.300812	-345.156625	-345.394164	-345.270036	0.131076
TSIc	-346.269059	-345.129453	-345.366423	-345.243901	0.128598
TSII	-346.301638	-345.158168	-345.395227	-345.271655	0.130245
TSIII	-346.305634	-345.158272	-345.394973	-345.272053	0.130987
TSIVa	-346.302714	-345.156450	-345.394920	-345.268984	0.130787
TSIVb	-346.273611	-345.131007	-345.368209	-345.244779	0.128809
TSV	-346.265083	-345.125061	-345.362029	-345.238420	0.129504
TSVI	-346.271694	-345.129392	-345.366131	-345.242646	0.129566
$CH_3\bullet$	-39.842880	-39.668728	-39.708648	-39.691041	0.029757
(CH₂OH structure)	-306.456068	-305.511248	-305.704887	-305.582361	0.094954
$HOCH_2\bullet$	-115.060788	-114.696253	-114.787210	-114.723899	0.037513
(structure)	-231.243804	-230.486112	-230.631089	-230.552585	0.089743
$CH_2=CH\bullet$	-77.906307	-77.603391	-77.656966	-77.648675	0.036643
(HOCH₂ structure)	-268.375801	-267.548525	-267.730032	-267.607604	0.089220
$CH_2=O$	-114.503199	-114.167414	-114.241678	-114.190322	0.026718
(structure)	-231.242235	-230.485145	-230.630207	-230.550761	0.089781
(structure)	-117.235736	-116.778956	-116.861863	-116.839269	0.065585
(CH₂OH structure)	-229.045593	-228.369889	-228.522326	-228.413240	0.061136
(OH structure)	-231.757723	-230.966675	-231.130141	-231.047642	0.100060
(OH structure)	-231.765032	-230.971152	-231.134773	-231.051712	0.099787

the geometry was optimized at the B3LYP/6-31G(d,p) level of theory and the transition state was searched using the same structure. The transition state structures were verified from the frequency calculations. For all the transition states identified, the calculated vibrational frequencies contained only one imaginary component, confirming the first-order saddle point

TS1a

OC$_2$C$_1$ = 115.9
OC$_2$C$_3$ = 121.6
OC$_2$C$_5$ = 98.6
C$_2$C$_3$C$_4$ = 122.2
OC$_2$C$_1$O = 29.8
OC$_2$..OH = -3.2

TS1b

C$_2$C$_5$ = 1.53
OC$_2$C$_1$ = 95.4
OC$_2$C$_3$ = 119.9
OC$_2$C$_5$ = 118.2
C$_2$C$_3$C$_4$ = 122.4
OC$_2$C$_1$ = 54.8
OC$_2$..OH = -4.6

TS4a

C$_3$C$_4$O = 101.6
OC$_3$C$_4$ = 97.9
OC$_3$C$_2$C$_5$ = -14.0
OC$_3$C$_4$O = -48.7
OC$_3$..OH = -3.3

TS4b

C$_3$C$_4$O = 108.1
OC$_3$C$_4$ = 119.9
OC$_3$C$_2$C$_5$ = -18.7
OC$_3$C$_4$O = -72.6
OC$_3$..OH = -5.0

Figure 3. Optimized geometries of the transition states of the C−C bond fission of the alkoxy radicals **I** and **IV** calculated at the B3LYP/6-31G(d,p) level of theory (bond lengths in Å and angles in deg).

TABLE 2: Reaction Enthalpies for the Alkoxy Radical Decomposition with Zero-Point Correction Included (kcal mol^{-1}).

reacn	B3LYP/ 6-31G(d,p)	MP2/ 6-31G(d)	MP2/ 6-311++G(d,p)	CCSD(T)/ 6-31G(d)	CCSD(T)/ 6-31G(d) + CF	CCSD(T)/ 6-311G(d,p)	B3LYP/ 6-31G(d)[a]
Ia	0.7	−2.9	−2.5	3.2	3.6		0.8
Ib	−1.3	−2.8	−3.9	2.8	1.8	2.1	−1.4
Ic	11.9	15.4	14.9	14.6	14.1		12.2
II	−10.7	−2.9	−4.7	−3.9	−5.6		−9.2
III	−5.8	−1.1	−2.6	−2.1	−3.5		−5.0
IVa	0.9	−4.7	−5.2	2.1	1.6		1.1
IVb	14.2	15.4	15.3	15.6	15.5		14.3
V	23.4	19.2	16.9	21.3	19.0		24.6
VI	18.0	15.1	12.8	18.0	15.6		20.1

[a] Taken from ref 18.

configuration. Spin contamination for all the transition states in geometry optimization using B3LYP is also low. The values of $\langle S**2 \rangle$ are less than 0.770 before projection and are very close to 0.750 after annihilation.

Figure 3 shows the transition state structures of radicals **I** and **IV** obtained at the B3LYP/6-31G(d,p) level of theory. As is seen from Figure 3, the lengths for breaking the C−C bond range from 2.00 to 2.24 Å. In addition, the intramolecular hydrogen bond is preserved in the transition states. Our structures of the transition states for the C−C fission of radicals **I−VI** obtained at the B3LYP/6-31G(d,p) level of theory are also similar to those obtained by Dibble, who reported the transition state structures using the B3LPY/6-311G(2df,2p) method.

We have obtained the energetics of the transition states and products of alkoxy radical decomposition using MP2 and CCSD(T) with different basis set sizes, to survey electron correlation and basis set effects. The absolute energies of those species are also presented in Table 1. Tables 2 and 3 summarize the reaction and activation enthalpies of the alkoxy radical decomposition, respectively. The results from Tables 2 and 3 indicate that the enthalpies of reaction and activation for the decomposition of the alkoxy radicals are very sensitive to the effect of electron correlation. For example, the reaction for

radical **I** to lose the •CH$_2$OH radical is slightly exothermic at the B3LYP/6-31G(d), MP2/6-31G(d), and MP2/311++G(d,p) levels of theory. However, using the CCSD(T) method with the basis set of 6-31G(d), this reaction is found to be endothermic by 2.8 kcal mol^{-1}. Similarly, our results indicate that the calculated activation barriers are also strongly dependent on the level of theory used. For the decomposition reaction **Ia**, the energy barrier obtained using the B3LYP/6-31G(d,p) is much smaller than that obtained using MP2 or CCST(T). In addition, at the MP2 level of theory, the effect of the basis set on the enthalpies of reaction and activation is not significant. The energy differences are within 2.3 kcal mol^{-1} between the basis sets 6-31G(d) and 6-311++G(d,p), smaller than the energy differences obtained using the different methods for electron correlation.

The basis set correction method discussed above was employed to determine the enthalpies of reaction and activation of the alkoxy radical decomposition, by correcting the CCSD(T)/ 6-31G(d) values with the correction factors developed at the MP2 level of theory. The reaction and activation enthalpies obtained at the CCSD(T)/6-31G(d) + CF level of theory are also included in Tables 2 and 3, respectively. In an effort to validate those values, we have conducted additional single-point

Hydroxyisoprene Alkoxy Radicals

J. Phys. Chem. A, Vol. 105, No. 15, 2001 **3813**

TABLE 3: Activation Enthalpies for the Alkoxy Radical Decomposition with Zero-Point Correction Included (kcal mol⁻¹).

reacn	B3LYP/ 6-31G(d,p)	MP2/ 6-31G(d)	MP2/ 6-311++G(d,p)	CCSD(T)/ 6-31G(d)	CCSD(T)/ 6-31G(d) + CF	CCSD(T)/ 6-311G(d,p)	B3LYP/ 6-31G(d)[a]
Ia	10.8	21.5	19.7	14.9	13.1		10.9
Ib	3.5	15.7	13.7	9.3	7.2	8.5	3.6
Ic	21.8	31.2	29.5	24.1	22.4		21.9
II	3.0	16.9	14.5	9.1	6.7		1.2
III	1.6	15.0	13.3	7.2	5.6		1.6
IVa	3.3	13.2	11.1	7.9	5.8		3.4
IVb	20.3	27.9	26.6	21.8	20.5		20.3
V	22.5	26.5	24.7	22.7	20.9		22.4
VI	17.8	22.8	21.2	19.5	17.9		18.2

[a] Taken from ref 18.

energy calculations for all the species associated with reaction **Ib** at the CCSD(T)/6-311G(d,p) level of theory; the values are also given in Tables 2 and 3. As is evident in the two tables, both reaction and activation enthalpies obtained using the methods of CCSD(T)/6-31G(d) + CF and CCSD(T)/6-311G(d,p) agree with 1.3 kcal mol⁻¹, confirming that the approach using the basis set correction factors yields satisfactory energetics. It should be pointed out that the single-point energy calculations of the alkoxy radicals at the CCSD(T)/6-311G(d,p) are extremely computational consuming. The execution of the single-point energy calculations for radical **I** and its corresponding transition state **TSIb** took 8 and 5 days of continuous CPU time, respectively, on our supercomputing system (granted by a special permission). Apparently, we were unable to perform calculations at such a level of theory for all the species reported in this work. We estimate an uncertainty of ±2 kcal mol⁻¹ associated with the energetics of the alkoxy radical decomposition reactions, on the basisi of a validation study of similar radical species and the comparison of the CCSD(T) results using the different basis sets as described above.[20,21]

Tables 2 and 3 show that at the CCSD(T)/6-31G(d) + CF level of theory the C−C fission is slightly endothermic for reactions **Ib** and **IVa** but is exothermic for **II** and **III**. Those decomposition pathways proceed with relatively small activation barriers, ranging from 5 to 8 kcal mol⁻¹. The decomposition of radical **I** to lose the methyl radical is slightly exothermic, with an activation barrier of about 13 kcal mol⁻¹. On the other hand, the decomposition pathways **Ic**, **IVb**, **V**, and **VI** are strongly endothermic (14−19 kcal mol⁻¹), with significant activation barriers of 17−23 kcal mol⁻¹.

A recent theoretical study has reported the reaction and activation enthalpies of C−C bond fission pathways of the hydroxyisoprene alkoxy radicals, using the B3LYP/6-31G(d) and B3LYP/6-311G(2df,2p) methods.[18] While our results obtained at the B3LYP/6-31G(d,p) level of theory closely resemble the previously reported using B3LYP/6-31G(d), our results obtained using CCSD(T) are noticeably different. In particular, there are significant differences between our CCSD-(T) results and those obtained before using B3LYP/6-311G-(2df,2p). For example, at the CCSD(T)/6-31G(d) + CF level of theory, our results predict that the decomposition reactions **Ib** and **IVa** are slightly endothermic, in contrast to the previous findings (with the exothermicity of 5.3 kcal mol⁻¹ for **Ib** and 2.8 kcal mol⁻¹ for **IVa** at the B3LYP/6-311G(2df,2p) level of theory).[18] In addition, the energy barriers that we obtain using CCSD(T)/6-31G(d) + CF are higher than those reported previously using B3LYP/6-311G(2df,2p), by 5.1 kcal mol⁻¹ for **Ia** and 3.7 kcal mol⁻¹ for **IVa**. Similarly, at the CCSD(T)/6-31G(d) + CF level of theory we calculated much larger energy barriers for reactions **II** and **III** than those reported before.[18] We noted that in the work of Dibble the energetics obtained using the 6-31G(d) basis set were preferred than those obtained
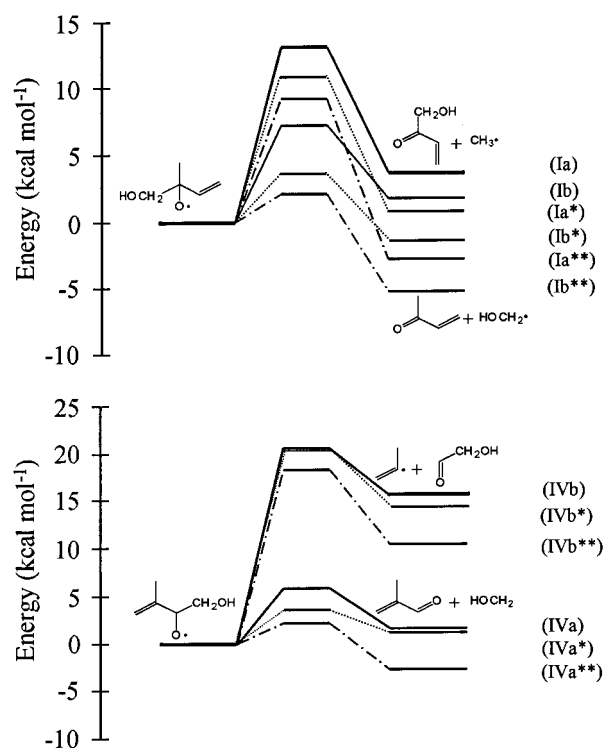
Figure 4. Potential energy surfaces for the C−C bond fission of radicals **I** and **IV** obtained at the CCSD(T)/6-31G(d) + CF//B3LYP/6-31G(d,f) level of theory. Also shown in this figure for comparison are energies reported in ref 18 using the B3LYP/6-31G(d) (with the pathways marked by an asterisk) and B3LYP/6-31G(2df,2p) (with the pathways marked by a double asterisk) levels of theory.

using the 6-311G(2df,2p) basis set,[18] on the basis of comparing computations to available experimental results of similar systems. In addition, the author suggested that his results could underestimate the true enthalpies by up to 2 kcal mol⁻¹. Figure 4 depicts the potential energy surfaces of the C−C bond fission for radicals **I** and **IV**, along with a comparison of the present results with those reported in ref 18.

Using the presently obtained activation energy barriers and the transition state theory (TST), we have calculated the high-pressure limit rate constants for the decomposition of the alkoxy radicals. The unimolecular decomposition rate is expressed by

$$k_{uni} = \frac{kT Q^{\mp}_{AB}}{h\, Q_{AB}} \exp\left(-\frac{\Delta E}{kT}\right) \qquad (4)$$

where $Q^{\mp}_{AB}$ is the partition function of the transition state with the vibrational frequency corresponding to the reaction coordinate removed, Q_{AB} is the partition function of the alkoxy radical, and ΔE is the zero-point corrected transition state energy relative to the separated products. The association rate can be

TABLE 4: Calculated High-Pressure Limit Unimolecular Decomposition Rate Constants of the Alkoxy Radicals, Association Rate Constants, and Equilibrium Constants[a]

reacn	k_{uni} (s^{-1})	k_{rec} (s^{-1})	K_{eq}
Ia	2.4×10^3	4.0×10^{-22}	1.7×10^{-25}
Ib	4.3×10^7	5.9×10^{-20}	1.4×10^{-27}
Ic	2.9×10^{-3}	2.5×10^{-21}	8.5×10^{-19}
II	1.3×10^8	6.6×10^{-25}	5.2×10^{-33}
III	6.0×10^8	9.1×10^{-23}	1.5×10^{-31}
IVa	3.1×10^8	9.8×10^{-19}	3.2×10^{-27}
IVb	4.9×10^{-2}	1.1×10^{-18}	2.2×10^{-17}
V	1.5×10^{-2}	1.0×10^{-16}	7.2×10^{-15}
VI	2.5×10^{-2}	3.6×10^{-17}	1.5×10^{-17}

[a] Rate constant calculations were performed on the basis of the CCSD(T)/6-31G(d) + CF//B3LPY/6-31G(d,p) level of theory.

obtained from the dissociation rate through the equilibrium constant

$$\frac{k_{rec}}{k_{uni}} = K_{eq} = \frac{Q_{AB}}{Q_A Q_B} \exp\left(\frac{\Delta E'}{kT}\right) \qquad (5)$$

where Q_A and Q_B are the partition functions of the individual products, and $\Delta E'$ is the zero-point corrected reaction energy. The partition functions required for eqs 4 and 5 were determined from unscaled vibrational frequencies and moments of inertia for the various species obtained from the DFT calculations at the B3LYP/6-31G(d,p) level of theory. The reaction energies were based on the calculations at the CCSD(T)/6-31G(d) + CF// B3LYP/6-31G(d,p) level.

The calculated high-pressure limit rate constants of decomposition of the alkoxy radicals and the corresponding recombination at 300 K are listed in Table 4. For radicals **I** and **IV**, the C−C bond fission to lose the •CH$_2$OH radical occurs with the rate constants of 4.3×10^7 and 3.1×10^8 s^{-1}, respectively. Reaction Ia to form the methyl radical has a much smaller rate of 2.4×10^3 s^{-1}. Table 4 also indicates that the association rates to re-form the alkoxy radicals are very slow. Hence for radicals **I** and **IV**, reactions Ib and IVa are dominant, despite their slight endothermicity. The C−C fission of radicals **II** and **III** is exothermic, with the energy barriers of 6.7 and 5.6 kcal mol^{-1}, respectively, at the CCSD(T)/6-31G(d) + CF level of theory. Hence those two reactions also occur readily, with the rate constants of 1.3×10^8 s^{-1} for **II** and 6.0×10^8 s^{-1} for **III**. On the other hand, the rate constants of the other decomposition channels (i.e., reactions Ic, IVb, V, and VI) of the alkoxy radicals are very small (i.e., $< 5 \times 10^{-2}$ s^{-1}). Note that the calculated rate constants are very sensitive to the determination of the activation barriers of the alkoxy radical decomposition. A variation of ±2 kcal mol^{-1} in the activation energy results in a change of a factor of 28 on the calculated rate constant. For reactions Ib, II, III, and IVa, our calculated decomposition rate constants are much smaller than those recently reported by Dibble,[18] who suggest the rate constants of the order of 10^{13} s^{-1} at 298 K. Apparently, the differences in the rate constants between the two studies can be explained by the fact that our activation barriers are higher obtained at the CCSD(T) level of theory. It should be pointed out that reaction 3, which proceeds through a hydroxy peroxynitrite intermediate, initially results in formation of vibrationally excited alkoxy radicals, with an exothermicity of about 10 kcal mol^{-1} on the basis of our ab initio calculations. The excited alkoxy radicals then decompose "promptly" by C−C bond rupture or are collisionally stabilized by the bath gas.[23] Our results suggest that the relaxed β-hydroxyalkoxy radicals readily undergo thermal decomposition. We are carrying out additional calculations to study the

structures of the hydroxy peroxynitrite intermediates and stabilization of the excited alkoxy radicals.

Atmospheric Implications. Our calculations using high-level ab initio theory suggest that thermal decomposition of the β-hydroxyalkoxy radicals occurs efficiently. For the four radicals **I−IV** the rates of decomposition are faster than their expected rates of 10^6 s^{-1} for isomerization and 4×10^4 s^{-1} for reaction with O$_2$.[9] Hence the C−C bond fission of those radicals will likely dominate the chemistry. On the other hand, decomposition of the two δ-hydroxyalkoxy radicals (**V and VI**) is unfavorable, due to the large activation barriers and strong endothermicity. Hence the C−C bond fission of those two radicals will be unimportant in the atmosphere. These conclusions are consistent with the recently suggested by Dibble,[18] although there are significant differences in the predicted enthalpies of reaction and activation as well as in the rate constants of the alkoxy radical decomposition reactions between the two studies. Another recent study has reported the isomeric branching ratios for the formation of the OH−O$_2$−isoprene peroxy radicals.[21] Those branching ratios are likely to be propagated to the corresponding alkoxy radicals,[15] resulting in values of 0.34: 0.02:0.05:0.29:0.22:0.08 for radicals **I−VI**. Hence the formation yields of alkoxy radicals **I** and **IV** (0.34 and 0.29) are much larger than those of radicals **II** and **III** (0.02 and 0.05).

Laboratory studies of the OH-initiated isoprene reactions in the presence of NO$_x$ have identified several major products, including methyl vinyl ketone (MVK) (36 ± 3%), methacrolein (MACR) (25 ± 3%), and formaldehyde (67 ± 7%), along with minor 3-methylfuran (4 ± 2%).[10−13] On the basis of the presently calculated rate constants, we conclude that MVK arises mainly from radical **I** via reaction Ib, while MCAR is produced primarily from radical **IV** via reaction IVa. Both reactions are also mainly responsible for the formation of formaldehyde. The fact that the earlier experiments observed a small yield for 3-methylfuran indicate relatively small branching ratios for the formation of radicals **II** and **III**, since radicals **II** and **III** may cyclize to form 3-methylfuran. Our earlier theoretical results predict that radicals **II** and **III** represent about 7% of the all the alkoxy radicals produced from the OH−isoprene reactions.[21,22] In addition, our rate calculations suggest a small rate for reaction **Ia** to lose the methyl radical, which may explain the identification of the carbonyl C$_4$H$_6$O$_2$ in a previous smog chamber investigation.[14]

Conclusions

In this study, we have presented DFT and ab initio molecular orbital calculations of the alkoxy radicals from the OH-initiated reaction of isoprene and their decomposition pathways. The geometries and energetics of the six isomers of the alkoxy radical and the transition states and products of their decomposition reactions have been investigated. The effects of electron correlation and basis set on the reaction and activation enthalpies for the C−C bond fission of the alkoxy radicals have been evaluated, indicating that the calculated energies are very sensitive to electron correlation effect. A computationally efficient method for calculating the energetics of the hydroxy-isoprene alkoxy radicals is presented. In addition, we have calculated the high-pressure limit rate constants of the C−C bond decomposition of the alkoxy radicals, using the presently obtained activation enthalpies and transition state theory (TST). The C−C bond fission occurs readily for the four β-hydroxy-alkoxy radicals with the calculated rate constants in the range of 4×10^7 to 6×10^8 s^{-1}, but this pathway is likely to be unimportant for the two δ-hydroxyalkoxy radicals. The results

Hydroxyisoprene Alkoxy Radicals

J. Phys. Chem. A, Vol. 105, No. 15, 2001 **3815**

suggest that thermal decomposition of the two β-hydroxyalkoxy radicals **I** and **IV** is mainly responsible for the formation of MVK, MACR, and formaldehyde under atmospheric conditions. Hence the present results provide further insight into the complex mechanism of atmospheric photochemical oxidation of isoprene.

References and Notes

(1) Rasmussen, R. A.; Khalil, M. A. *J. Geophys. Res.* **1988**, *93*, 1417.

(2) Trainer, M.; et al. *Nature* **1987**, *329*, 705.

(3) Placet, M.; Battye, R. E.; Fehsenfeld, F. C.; Bassett, G. W. In *NAPAP SOST Report 1, National Acid Precipitation Assessment Program*; Washington, DC, 1990.

(4) Atkinson, R. *J. Phys. Chem. Ref. Data* **1997**, *26*, 251.

(5) Seinfeld, J. H.; Pandis, S. N. *Atmospheric Chemistry and Physics: From Air Pollution to Climate Change*; John Wiley & Sons: New York, 1997.

(6) Chameides, W. L.; Lindsay, R. W.; Richardson, J.; Kiang, C. S. *Science* **1988**, *241*, 1473.

(7) Jacob, D. J.; Wofsy, S. C. *J. Geophys. Res.* **1988**, *93*, 1477.

(8) Zhang, R.; Suh, I.; Clinkenbeard, A.; Lei, W.; North, S. W. *J. Geophys. Res.* **2000**, *105*, 24627.

(9) Atkinson, R. *Int. J. Chem. Kinet.* **1997**, *29*, 99.

(10) Atkinson, R.; Aschmann, S. M.; Winer, A. M.; Pitts, J. N., Jr. *Int. J. Chem. Kinet.* **1982**, *14*, 507.

(11) Tuazon, E. C.; Atkinson, R. *Int. J. Chem. Kinet.* **1990**, *22*, 1221.

(12) Paulson, S. E.; Seinfeld, J. H. *Int. J. Chem. Kinet.* **1992**, *24*, 79.

(13) Paulson, S. E.; Seinfeld, J. H. *J. Geophys. Res.* **1992**, *97*, 20703.

(14) Yu, J.; Jeffries, H. E.; Le Lacheur, R. M. *Environ. Sci. Technol.* **1995**, *29*, 1923.

(15) Jenkin M. E.; Hayman, G. D. *J. Chem. Soc., Faraday Trans.* **1995**, *91*, 1911.

(16) Jenkin, M. E.; Boyd, A. A.; Lesclaux, R. *J. Atmos. Chem.* **1998**, *29*, 267.

(17) Carter, W. P. L. *Atmos. Environ.* **1996**, *30*, 4275.

(18) Dibble, T. S. *J. Phys. Chem.* **1999**, *103*, 8559.

(19) Frisch, M. J.; Trucks, G. W.; Schlegel, H. B.; Gill, P. M. W.; Johnson, B. G.; Robb, M. A.; Cheeseman, J. R.; Keith, T.; Petersson, G. A.; Montgomery, J. A.; Raghavachari, K.; Al-Laham, M. A.; Zakrzewski, V. G.; Ortiz, J. V.; Foresman, J. B.; Cioslowski, J.; Stefanov, B. B.; Nanayakkara, A.; Challacombe, M.; Peng, C. Y.; Ayala, P. Y.; Chen, W.; Wong, M. W.; Andres, J. L.; Replogle, E. S.; Gomperts, R.; Martin, R. L.; Fox, D. J.; Binkley, J. S.; Defrees, D. J.; Baker, J.; Stewart, J. P.; Head-Gordon, M.; Gonzalez, C.; Pople, J. A. *Gaussian 98*, revision D.3; Gaussian, Inc.: Pittsburgh, PA, 1998.

(20) Lei, W.; Derecskei-Kovacs, A.; Zhang, R. *J. Chem. Phys.* **2000**, *113*, 5354.

(21) Lei, W.; Zhang, R.; McGivern, W. S.; Derecskei-Kovacs, A.; North, S. W. *J. Phys. Chem.* **2001**, *105*, 471.

(22) Lei, W.; Zhang, R.; McGivern, W. S.; Derecskei-Kovacs, A.; S. W. North, *Chem. Phys. Lett.* **2000**, *326*, 109.

(23) Orlando, J. J.; Tyndall, G. S.; Bilde, M.; Ferronato, C.; Wallington, T. J.; Vereecken, L.; Peeters, J. *J. Phys. Chem.* **1998**, *102*, 8116.